Received 28 February 2024, accepted 19 March 2024, date of publication 25 March 2024, date of current version 29 March 2024.

Digital Object Identifier 10.1109/ACCESS.2024.3381525

RESEARCH ARTICLE

Improvement of Retention Characteristics Using Doped SiN Layer Between WL Spaces in 3D NAND Flash

HYEWON KYUNG[1,4], YUNEJAE SUH[2,4], YOUNGHO JUNG[3], AND DAEWOONG KANG[4]

[1]School of Electrical and Electronics Engineering, Chung-Ang University, Seoul 06974, Republic of Korea
[2]Department of Electronic Engineering, Soongsil University, Seoul 06978, Republic of Korea
[3]Department of Electronic and Electrical Engineering, Daegu University, Gyeongsan, Gyeongbuk 38453, Republic of Korea
[4]Next Generation Semiconductor Convergence and Open Sharing System, Seoul National University, Seoul 08826, Republic of Korea

Corresponding authors: Youngho Jung (05jung@daegu.ac.kr) and Daewoong Kang (freekite@snu.ac.kr)

This work was supported by Daegu University Research under Grant 20200262.

ABSTRACT We propose a novel structure of a charge trapping layer, that is doped between Word Line(WL) spaces in 3D NAND flash memory. To estimate the retention characteristics, the ΔV_{th} of each structure by doping type is compared to a reference structure during retention operation. In this study, lateral charge spreading, rather than vertical loss, is mainly studied as an indicator to determine how long stored data can survive on the selected cell. When the SiN layer is doped with p-type, the electrostatic potential decreases and SRH recombination increases in the doping region. As a result, the p-type doping structure has better retention characteristics than others. In addition, for an optimized structure between retention characteristics and cell current, the doping region of the SiN layer is split and analyzed by the thickness of the doping region. Since the p-type doping region is thicker, lateral spreading is effectively blocked although the cell current decreased slightly.

INDEX TERMS 3D NAND, doped SiN layer, electrostatic potential, lateral charge spreading, SRH recombination.

I. INTRODUCTION

The advancement of NAND flash memory from a 2D planar structure to a 3D vertical structure enables faster speed at a lower cost, higher density, and scaling down. Although 3D NAND charge trap flash(CTF) has many advantages and applications [1], [2], [3], [4], [5], there is a critical problem caused by sharing the charge trap flash (CTL) of the target cell with adjacent cells [6], [7], [8], [9], [10], [11]. In CTL, there is charge loss during retention operations, due to vertical loss and lateral charge spreading. The cause of vertical loss is the trapped charges of nitride passing through the tunneling oxide [12], [13], [14]. Lateral charge spreading is caused by the electric field [15], [16] from charges in WL spaces and adjacent cells. Charge loss has a greater impact on 3D NAND flash memory as it is scaled down, and there is a steady stream of research about this [17], [18], [19], [20], [21], [22]. In this work, we propose a new structure of 3D NAND CTF with thin doping in the SiN layer (CTL) between WL spaces using high SiN/SiO_2 etching selectivity [23]. These doped regions in the SiN layer reduce the impact of the electric field causing lateral charge spreading. The study consists of two parts, a comparison of characteristics by doping type and by doping thickness. In the first part about doping type, we show which doping type in SiN improves the retention characteristics. Then, in the second part about doping thickness, the optimal doping thickness is found using the relationship between the retention characteristics and the cell current.

The associate editor coordinating the review of this manuscript and approving it for publication was Yu Liu.

II. PROPOSED STRUCTURE

Fig. 1 (a) shows a cross-sectional view of 3D NAND flash memory created by TCAD Sentaurus Device Editor(SDE) [24], [25]. It consists of 3 WLs, an ONO stack, a polysilicon channel, a source, a drain, and an oxide filler. The O/N(=Oxide/Nitride) pitch of the word line is 50 nm for 25 nm. The oxide and SiN layer thicknesses of the ONO stack

© 2024 The Authors. This work is licensed under a Creative Commons Attribution-NonCommercial-NoDerivatives 4.0 License.
For more information, see https://creativecommons.org/licenses/by-nc-nd/4.0/

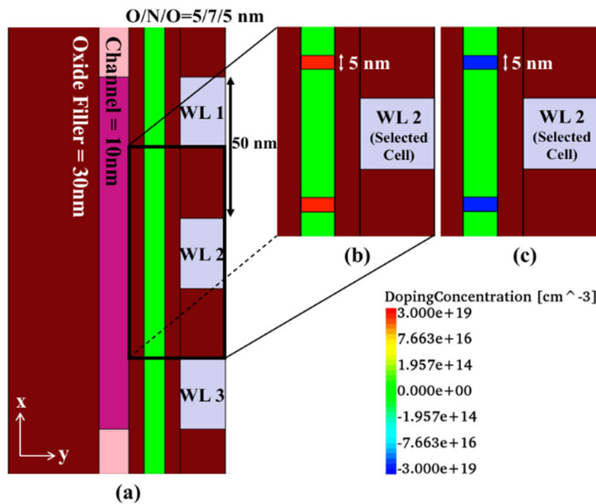

FIGURE 1. (a) Cross-sectional view of reference structure with 3 WLs in 3D NAND flash memory used in TCAD simulation (b) Proposed 3D NAND structure with N-doping in the SiN layer and (c) P-doping in the SiN layer.

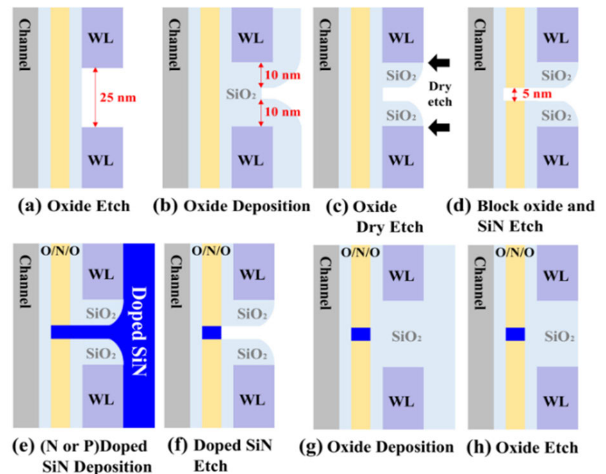

FIGURE 2. Manufacturing process of 3D NAND flash structures with doped SiN layer.

TABLE 1. Conditions for TCAD simulation.

	B/L	Selected cell	Unselected cell	Temperature
Erase	0 V	-18 V	0 V	-
Program	0 V	18 V	7 V	-
Read	0 to 0.5 V	-5 to 10 V	7 V	-
Retention	0 V	0 V	0 V	300 K

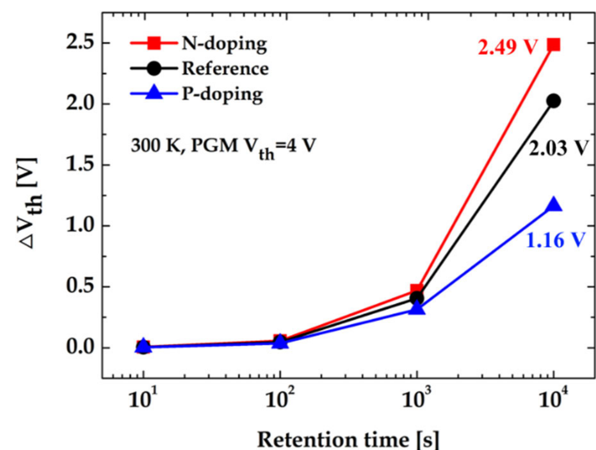

FIGURE 3. Comparison of ΔV_{th} (= |Vth_retention-Vth_program|) as a function of retention time and doping type in the SiN layer.

are 5 nm and 7 nm, respectively. The source on the bottom of the channel and drain on top of the channel are doped with phosphorus 5×10^{18} cm^{-3} and a channel is doped with boron 1×10^{15} cm^{-3}. The SiN layer of the ONO stack between WL spaces is doped with phosphorus in Fig. 1 (b) and boron in Fig. 1 (c). The doping concentration is both 3×10^{19} cm^{-3} which is the same value as the trap concentration of the SiN layer set in the TCAD simulation. The length of doping in SiN is 5 nm in the x-direction, and the thickness of doping in SiN is 7 nm in the y-direction.

Fig. 2 illustrates the manufacturing process of proposed 3D NAND flash structures in Fig. 1 (b) and (c), which incorporate doped SiN regions. In Fig. 2 (b) and (c), a 10 nm oxide layer is uniformly deposited and etched using dry etching techniques [26]. Moving on to Fig. 2 (d), the SiN is ultimately etched by 5 nm in the x-direction. For the deposition and etch process of oxide and SiN, thin and uniform structures between cells can be created with control of elaborate process conditions such as ALD cycle or etch rate [27], [28]. In Fig. 2 (e), the doped SiN layer is deposited using PECVD or ALD [29], [30], [31], [32] with uniform distribution. For this process, diborane or phosphine can be introduced into the chamber as dopants for N and P-doped SiN layer.

Threshold voltage (V_{th}) is measured with a constant current method with 100 nA. The nonlocal tunneling model is used between the channel and tunneling oxide. Also, the Poole-Frenkel effect for trap-assisted electron transport and Shockley-Read-Hall (SRH) recombination model for trap-assisted recombination are applied. The operation conditions for erase, program and read are shown in Table 1.

III. RESULTS AND DISCUSSION

A. TYPES OF DOPING

Fig. 3 shows the results of ΔV_{th} over a retention time at 300 K as a parameter of the doping types in the SiN. The program V_{th} of selected WL cell is set to 4 V and erase V_{th} of unselected WL cells is set to -1 V. Three types of structures were introduced including the reference, n-type doping and p-type doping in Fig. 1. The reference of Fig. 1 (a) is the basic structure of 3D NAND flash to compare data with doped structures in Fig. 1 (b) and (c). Fig. 3 shows the retention characteristics from 10 s to 10^4s. As doping types between WLs space change from n-doping to p-doping, it is confirmed that the retention characteristics are improved as shown in Fig. 3.

This result can be explained by the electrostatic potential in the SiN layer at retention time (10 s) as shown in Fig. 4 (a)

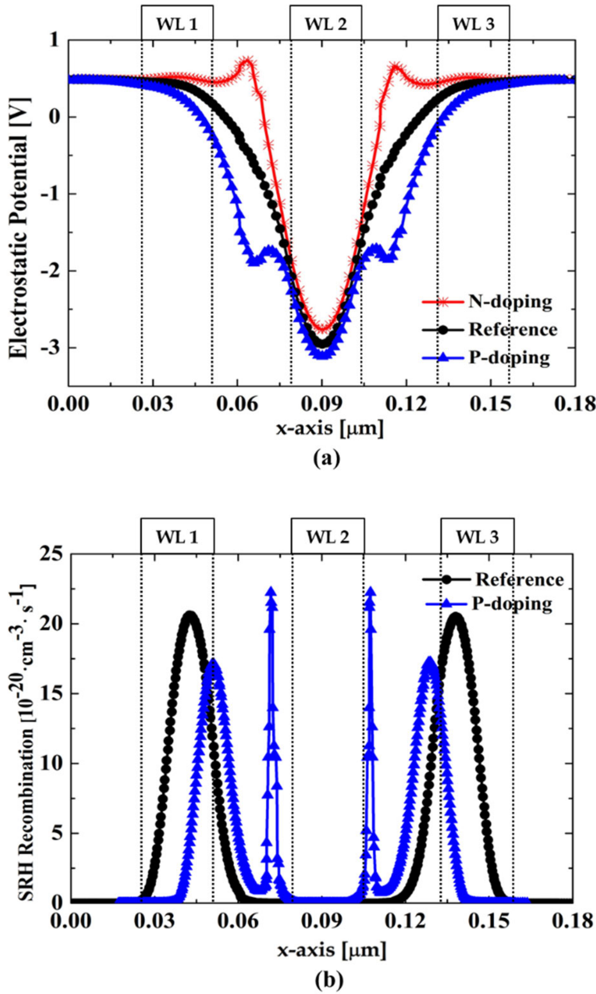

FIGURE 4. (a) Electrostatic potential of SiN layer and (b) SRH recombination of SiN layer according to x-axis for retention time=10 s.

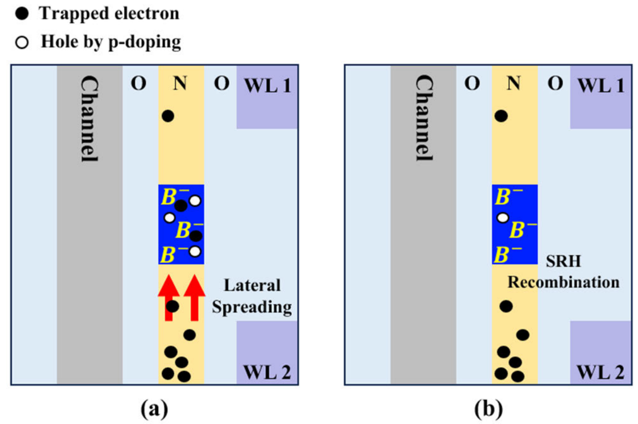

FIGURE 5. (a) Description of lateral spreading during the retention operation in the p-type doping structure 3D NAND flash memory. (b) Description of SRH recombination of SiN layer between spreading electrons and holes by p-type doping.

that decreases rapidly in the p-type doping region compared to others during the retention operation. These changes of potential affect lateral spreading. Therefore, electrons trapped for selected cells spread less to adjacent cells due to reduced potential in the p-type doping region. On the contrary, electrons for selected cells spread more to adjacent cells due to increased potential in the n-type doping region. Fig. 4 (b) shows SRH recombination in the SiN layer under the same conditions as shown in Fig. 4 (a). In particular, SRH recombination occurs in unselected cells and p-type doping region. Because many holes exist in the SiN layer in erased WL 1 and WL 3, they contribute to recombination in SiN layer of unselected cells.

Fig. 5 describes the lateral spreading of trapped electron and SRH recombination in the SiN layer during retention operation. In Fig. 5 (a), the trapped electrons in a selected cell(WL 2) move to unselected cells(WL 1 and WL 3) during the retention operation, and they pass through the p-type doping region. As recombination occurs between moving electrons and holes by p-type doping in Fig. 5 (b), the number of electrons spreading to the adjacent cells decreases, which means that the retention characteristics were improved. As a result, the difference between ΔV_{th} of p-type (=1.16 V) and ΔV_{th} of reference (=2.03 V) in Fig. 3 is 0.87 V after 10^4 s of retention. That is almost twice the difference between ΔV_{th} of n-type(=2.49 V) and ΔV_{th} of reference(=2.03 V), which is 0.46 V. The reason is that the n-type doping structure is only affected by potential, but the p-type doping structure is affected by both decreased potential and increased SRH recombination in doping regions. Therefore, the retention characteristics for the p-type doping structure are effectively improved.

Fig. 6 (a), (b), and (c) show electron trapped charge distribution in the SiN layer after program operation in n-type doping, reference, and p-type doping structures, respectively. Even if p-type doping structure has the least number of trapped electrons, it shows the largest V_{th} by a small difference when program voltage changes from 20 V to 26 V as shown in Fig. 6 (d). This result can be explained with Fig. 5. In Fig. 5 (a), there are the same number of acceptors (boron) and holes in the p-type doping region by ionization [33], [34]. As the lateral spreading of electrons occurs, the number of holes decreases due to recombination as shown in Fig. 5 (b). Therefore, p-type doping region has a negative charge due to more acceptors. This causes higher threshold voltage for the read operation and also affects the cell current as shown in Fig. 7. Even if p-doping structure shows the smallest cell current, the difference between reference and p-doping structure is negligible, which is about 0.2 mA/μm.

B. THICKNESS OF DOPING

In the previous study on types of doping, p-type doping structure had the best retention characteristics, but the cell current characteristics were degraded. The thinner a p-type doping region is, the less it is affected by the acceptor which means that it is good to improve cell current. In addition, it is more effective for the doping region to be located on the right side of the SiN layer based on Fig. 8. Fig. 8 shows the E-Field distribution of the reference structure during the retention

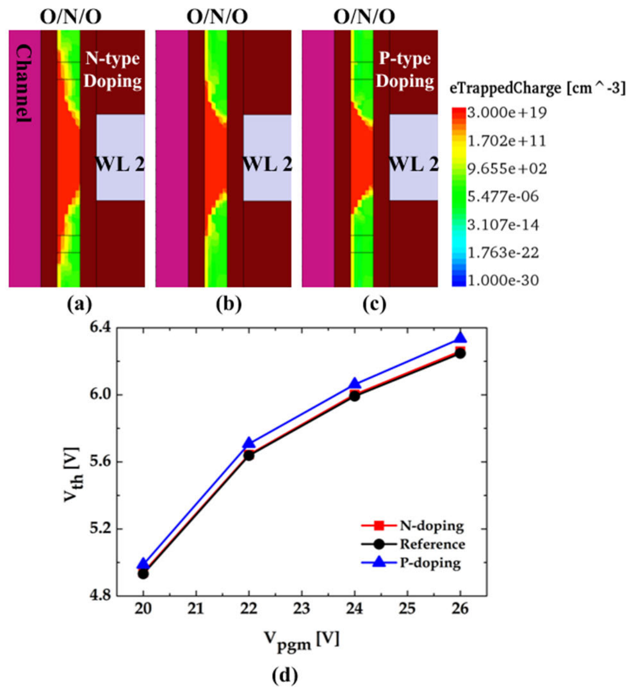

FIGURE 6. Electron trapped charge distribution in the SiN layer after the program of (a) n-doping in SiN, (b) reference, and (c) p-doping in SiN structures. (d) Comparison of V_{th} as a function of doping type in the SiN layer and program voltage from 20 V to 26 V.

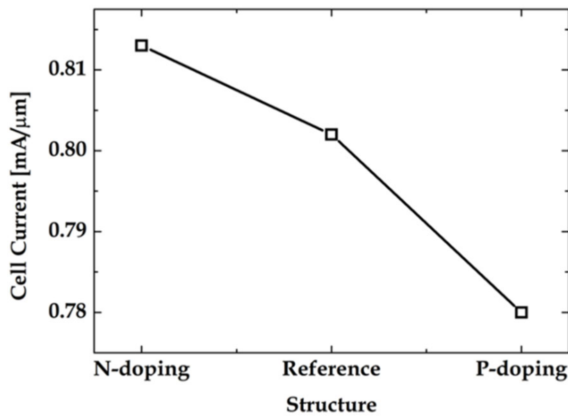

FIGURE 7. Cell current according to doping type in the SiN layer for drain voltage=9 V.

operation. Fig. 9 (a) and (b) show the charge distribution where the retention time is 10 s and 10^4 s, respectively. Fig. 9 (c) shows the electron trapped charge in the SiN layer along the line from point A to B in Fig. 9 (a) and (b). It is observed that lateral spreading occurs more on the right side near point B than the left side near point A in SiN as a stronger electric field is formed on the right side of SiN in Fig. 8.

For the optimized point, the thickness of the p-doping region is split in the y-direction from 1 nm to 7 nm in Fig. 10. The SiN layer is doped from the right side to the left side to effectively block lateral spreading using the minimum thickness of the doping region. Fig. 11 shows the results of ΔV_{th} over retention time at 300 K as a parameter of the doping thickness in the SiN. It is observed that the slope

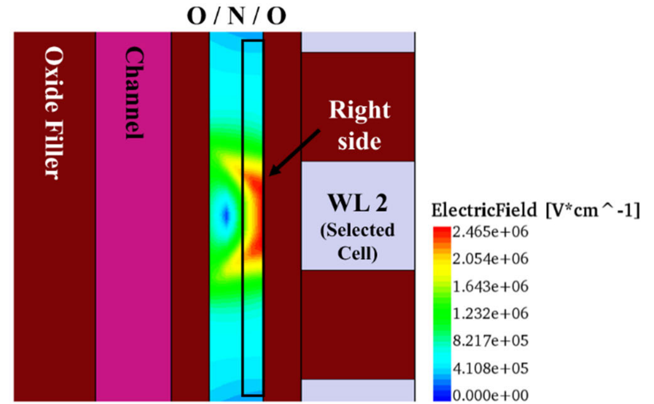

FIGURE 8. Schematic(TCAD) of electric field in the SiN layer during the retention operation at retention time=10 s in the reference structure.

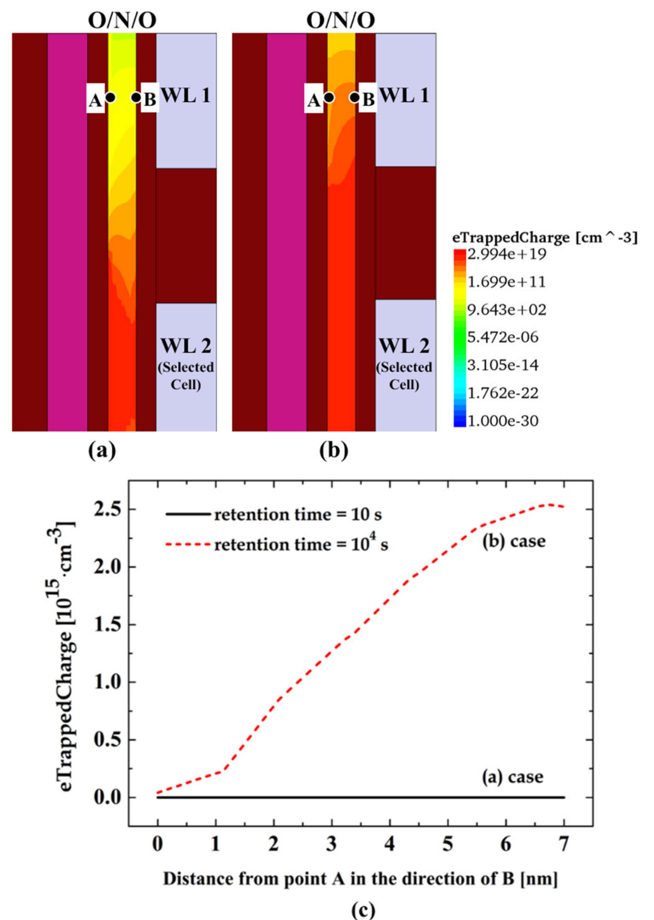

FIGURE 9. (a) Schematic(TCAD) of charge distribution in the reference structure for retention time=10 s and (b) 10000 s. (c) electron trapped charge in SiN as a function of distance from point A in the direction of B of Fig. 9 (a) and (b).

decreases at a slower rate as the doping region becomes thicker. Fig. 12 shows the p-type doping region's thickness window between $1/\Delta V_{th}$ using the data of Fig. 11 and the cell current estimated where the drain voltage is 9 V. The $1/\Delta V_{th}$ increases about 58 % under the condition of 7 nm thickness compared to 1 nm, while the cell current decreases only about 2 %, which is negligible. As a result, the best

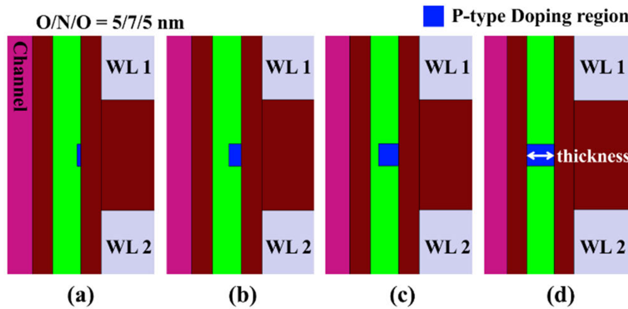

FIGURE 10. Schematic(TCAD) with variations of thickness of the p-type doping region in SiN for (a) 1 nm, (b) 3 nm, (c) 5 nm, and (d) 7 nm.

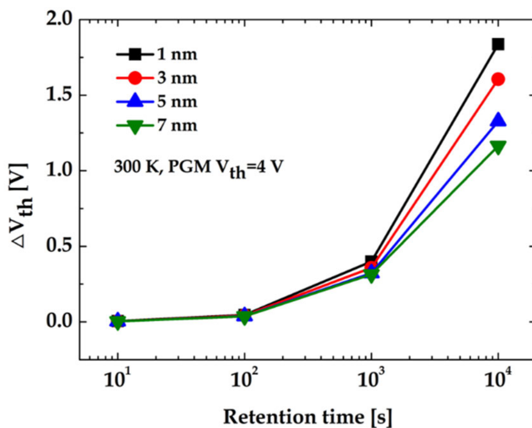

FIGURE 11. Comparison of ΔV_{th} (= |Vth_retention-Vth_program|) as a function of retention time and doping thickness in the SiN layer.

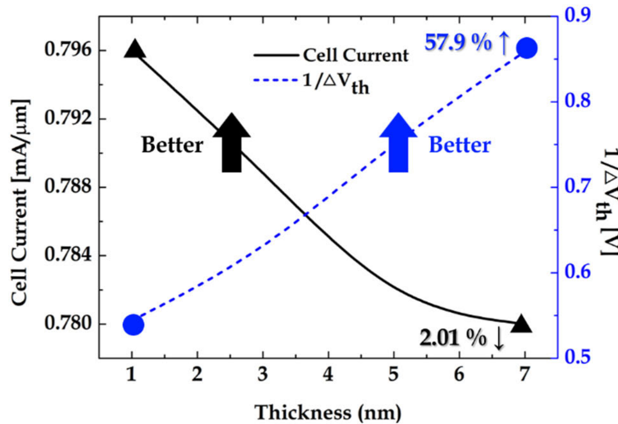

FIGURE 12. Cell current for 9 V of drain voltage and $1/\Delta V_{th}$ with the variation of the thickness of the p-type doping region of SiN layer.

window for thickness of the p-type doping region is between 3 nm and 4 nm considering both the retention characteristics and the cell current.

IV. CONCLUSION

A new structure using the doped SiN layer of 3D NAND flash was proposed. The p-type doping structure has the best retention characteristic of three structures: reference (Fig. 1 (a)), n-doping (Fig. 1 (b)), and p-doping (Fig. 1 (c)), due to decreased potential and increased SRH recombination of holes in the doping region. This effectively reduces lateral charge spreading from a selected cell to adjacent cells. On the other hand, p-doping structure degrades the cell current due to more acceptors as we discussed earlier. To solve this problem, an additional simulation was performed which shows the trade-off between cell current and retention characteristics. Finally, we found out the optimal thickness of p-doping region, which is between 3 nm to 4 nm, to meet proper cell current and retention characteristics.

REFERENCES

[1] Y. J. Song, J. H. Lee, H. C. Shin, K. H. Lee, K. Suh, J. R. Kang, S. S. Pyo, H. T. Jung, S. H. Hwang, G. H. Koh, S. C. Oh, S. O. Park, J. K. Kim, J. C. Park, J. Kim, K. H. Hwang, G. T. Jeong, K. P. Lee, and E. S. Jung, "Highly functional and reliable 8 Mb STT-MRAM embedded in 28 nm logic," in *IEDM Tech. Dig.*, Dec. 2016, pp. 27.2.1–27.2.4.

[2] K. Parat and A. Goda, "Scaling trends in NAND flash," in *IEDM Tech. Dig.*, Dec. 2018, pp. 2.1.1–2.1.4.

[3] M. Zhang, F. Wu, X. Chen, Y. Du, W. Liu, Y. Zhao, J. Wan, and C. Xie, "RBER aware multi-sensing for improving read performance of 3D MLC NAND flash memory," *IEEE Access*, vol. 6, pp. 61934–61947, 2018.

[4] R. Ma, F. Wu, M. Zhang, Z. Lu, J. Wan, and C. Xie, "RBER-aware lifetime prediction scheme for 3D-TLC NAND flash memory," *IEEE Access*, vol. 7, pp. 44696–44708, 2019.

[5] S.-T. Lee, D. Kwon, H. Kim, H. Yoo, and J.-H. Lee, "NAND flash based novel synaptic architecture for highly robust and high-density quantized neural networks with binary neuron activation of (1, 0)," *IEEE Access*, vol. 8, pp. 114330–114339, 2020.

[6] K. Lee, M. Kang, S. Seo, D. H. Li, J. Kim, and H. Shin, "Analysis of failure mechanisms and extraction of activation energies (E_a) in 21-nm NAND flash cells," *IEEE Electron Device Lett.*, vol. 34, no. 1, pp. 48–50, Jan. 2013.

[7] K. Lee, D. Kang, H. Shin, S. Kwon, S. Kim, and Y. Hwang, "Analysis of failure mechanisms in erased state of sub 20-nm NAND flash memory," in *Proc. 44th Eur. Solid State Device Res. Conf. (ESSDERC)*, Sep. 2014, pp. 58–61.

[8] D. Kang, K. Lee, S. Kwon, S. Kim, Y. Hwang, and H. Shin, "Analysis of read disturbance mechanism in retention of sub-20 nm NAND flash memory," *Jpn. J. Appl. Phys.*, vol. 54, no. 4S, Apr. 2015, Art. no. 04DD03.

[9] D. Kang, K. Lee, S. Seo, S. Kim, J.-S. Lee, D.-S. Bae, D. H. Li, Y. Hwang, and H. Shin, "Generation dependence of retention characteristics in extremely scaled NAND flash memory," *IEEE Electron Device Lett.*, vol. 34, no. 9, pp. 1139–1141, Sep. 2013.

[10] D. Kang, K. Lee, M. Kang, S. Seo, D. H. Li, Y. Hwang, and H. Shin, "Probability level dependence of failure mechanisms in sub-20 nm NAND flash memory," *IEEE Electron Device Lett.*, vol. 35, no. 3, pp. 348–350, Mar. 2014.

[11] S. J. Wrazien, Y. Zhao, J. D. Krayer, and M. H. White, "Characterization of SONOS oxynitride nonvolatile semiconductor memory devices," *Solid-State Electron.*, vol. 47, no. 5, pp. 885–891, May 2003.

[12] A. Maconi, A. Arreghini, C. M. Compagnoni, G. Van Den Bosch, A. S. Spinelli, J. Van Houdt, and A. L. Lacaita, "Comprehensive investigation of the impact of lateral charge migration on retention performance of planar and 3D SONOS devices," *Solid-State Electron.*, vol. 74, pp. 64–70, Aug. 2012.

[13] L. Liu, A. Arreghini, G. Van Den Bosch, L. Pan, and J. Van Houdt, "Assessment methodology of the lateral migration component in data retention of 3D SONOS memories," *Microelectron. Rel.*, vol. 54, nos. 9–10, pp. 1697–1701, Sep. 2014.

[14] M. C. Lee and H. Y. Wong, "Charge loss mechanisms of nitride-based charge trap flash memory devices," *IEEE Trans. Electron Devices*, vol. 60, no. 10, pp. 3256–3264, Oct. 2013.

[15] J. Lee, J. Seo, J. Nam, Y. Kim, K.-W. Song, J. H. Song, and W. Y. Choi, "Electric field impact on lateral charge diffusivity in charge trapping 3D NAND flash memory," in *Proc. IEEE Int. Rel. Phys. Symp. (IRPS)*, Dallas, TX, USA, Mar. 2022, pp. P29-1–P29-5.

[16] Y.-H. Liu, C.-M. Jiang, W.-C. Chen, T. Wang, W.-J. Tsai, T.-C. Lu, K.-C. Chen, and C.-Y. Lu, "Electric field induced nitride trapped charge lateral migration in a SONOS flash memory," *IEEE Electron Device Lett.*, vol. 38, no. 1, pp. 48–51, Jan. 2017.

[17] H.-J. Kang, N. Choi, D. H. Lee, T. Lee, S. Chung, J.-H. Bae, B.-G. Park, and J.-H. Lee, "Space program scheme for 3-D NAND flash memory specialized for the TLC design," in *Proc. IEEE Symp. VLSI Technol.*, Jun. 2018, pp. 201–202.
[18] C. Kang, J. Choi, J. Sim, C. Lee, Y. Shin, J. Park, J. Sel, S. Jeon, Y. Park, and K. Kim, "Effects of lateral charge spreading on the reliability of TANOS (TaN/AlO/SiN/oxide/Si) NAND flash memory," in *Proc. 45th Annu. IEEE Int. Rel. Phys. Symp.*, Phoenix, AZ, USA, Apr. 2007, pp. 167–170.
[19] Y. H. Liu, T. C. Zhan, Y. S. Yang, C. C. Hsu, A. C. Liu, and W. Lin, "Impact of trapped charge vertical loss and lateral migration on lifetime estimation of 3-D NAND flash memories," in *Proc. IEEE Int. Rel. Phys. Symp. (IRPS)*, Monterey, CA, USA, Mar. 2023, pp. 1–6.
[20] J. Park, G. Yoon, D. Go, D. Kim, U. An, J. Kim, J. Kim, and J.-S. Lee, "Decomposition of vertical and lateral charge loss in long-term retention of 3-D NAND flash memory," in *Proc. IEEE Int. Rel. Phys. Symp. (IRPS)*, Monterey, CA, USA, Mar. 2023, pp. 1–4.
[21] F. Wang, Y. Li, X. Ma, and J. Chen, "Charge loss induced by defects of transition layer in charge-trap 3D NAND flash memory," *IEEE Access*, vol. 9, pp. 47391–47398, 2021.
[22] H.-N. Yoo, B. Choi, J.-W. Back, H.-J. Kang, E. Kwon, S. Chung, J.-H. Bae, B.-G. Park, and J.-H. Lee, "Effect of lateral charge diffusion on retention characteristics of 3D NAND flash cells," *IEEE Electron Device Lett.*, vol. 42, no. 8, pp. 1148–1151, Aug. 2021.
[23] T. Kim, T. Park, and S. Lim, "Improvement of Si_3N_4/SiO_2 etching selectivity through the passivation of SiO_2 surface in aromatic carboxylic acid-added H_3PO_4 solutions for the 3D NAND integration," *Appl. Surf. Sci.*, vol. 619, May 2023, Art. no. 156758.
[24] Z. Lun, S. Liu, Y. He, Y. Hou, K. Zhao, G. Du, X. Liu, and Y. Wang, "Investigation of retention behavior for 3D charge trapping NAND flash memory by 2D self-consistent simulation," in *Proc. Int. Conf. Simul. Semiconductor Processes Devices (SISPAD)*, Sep. 2014, pp. 141–144.
[25] C. Woo, S. Kim, J. Park, D. Lee, M. Kang, J. Jeon, and H. Shin, "Modeling of lateral migration mechanism during the retention operation in 3D NAND flash memories," in *Proc. Electron Devices Technol. Manuf. Conf. (EDTM)*, Mar. 2019, pp. 261–263.
[26] Z. Chen, F. Fishburn, C. S. Kang, S. Varghese, and B. Haran, "Materials enabled memory scaling and new architectures," in *Proc. IEEE Int. Memory Workshop (IMW)*, Monterey, CA, USA, May 2023, pp. 1–4.
[27] W. J. Lee, U. J. Kim, C. H. Han, M. H. Chun, S. K. Rha, and Y. S. Lee, "Characteristics of silicon nitride thin films prepared by using alternating exposures of SiH_2Cl_2 and NH_3," *JKPS*, vol. 47, p. A598, Nov. 2004.
[28] X. Meng, Y.-C. Byun, H. Kim, J. Lee, A. Lucero, L. Cheng, and J. Kim, "Atomic layer deposition of silicon nitride thin films: A review of recent progress, challenges, and outlooks," *Materials*, vol. 9, no. 12, p. 1007, Dec. 2016.
[29] Y. K. Fang, C. F. Huang, C. Y. Chang, and R. H. Lee, "Preparation and characterization of boron- and phosphorus-doped hydrogenated amorphous silicon nitride films," *J. Electrochem. Soc.*, vol. 132, no. 5, p. 1222, 1985.
[30] H. Wang, C. Chen, M. Pan, Y. Sun, and X. Yang, "Light-induced enhancement of the minority carrier lifetime in boron-doped Czochralski silicon passivated by doped silicon nitride," *Appl. Surf. Sci.*, vol. 357, pp. 1991–1995, Dec. 2015.
[31] B. Macco, M. L. van de Poll, B. W. H. van de Loo, T. M. P. Broekema, S. B. Basuvalingam, C. A. A. van Helvoirt, W. J. H. Berghuis, R. J. Theeuwes, N. Phung, and W. M. M. Kessels, "Temporal and spatial atomic layer deposition of Al-doped zinc oxide as a passivating conductive contact for silicon solar cells," *Sol. Energy Mater. Sol. Cells*, vol. 245, Sep. 2022, Art. no. 111869.
[32] S. Gall, B. Paviet-Salomon, J. Lerat, and T. Emeraud, "Laser doping strategies using SiN:P and SiN:B dielectric layers for profile engineering in high efficiency solar cell," *Energy Proc.*, vol. 27, pp. 449–454, Jan. 2012.
[33] F. Oba, K. Tatsumi, H. Adachi, and I. Tanaka, "*n*- and *p*-type dopants for cubic silicon nitride," *Appl. Phys. Lett.*, vol. 78, no. 11, pp. 1577–1579, Mar. 2001.
[34] Z. Mao, Y. Zhu, Y. Zeng, F. Xu, Z. Liu, G. Ma, Z. Du, and W. Geng, "Investigation of al-doped silicon nitride-based semiconductor and its shrinkage mechanism," *CrystEngComm*, vol. 14, no. 23, pp. 7929–7933, 2012.

HYEWON KYUNG was born in Ulsan, South Korea, in 2001. She is currently pursuing the B.S. degree in electrical and electronics engineering from Chung-Ang University, Seoul, South Korea. Her research interests include process design of device with TCAD simulation and the reliability of 3-D NAND flash memory.

YUNEJAE SUH was born in Seoul, South Korea, in 1998. He is currently pursuing the B.S. degree in electronic engineering with Soongsil University, Seoul. His research interests include device design with TCAD simulation and characterization of 3-D NAND flash memory.

YOUNGHO JUNG received the B.S. degree in electronics engineering from Dongguk University, Seoul, South Korea, in 2005, the M.S. degree from Seoul National University, Seoul, in 2007, and the Ph.D. from Oregon State University, Corvallis, OR, USA, in 2014. His doctoral research was in wide band and high accuracy $\Delta\Sigma$ ADC. From 2007 to 2009, he was a Graphics Memory Design Engineer with SK-Hynix Semiconductor, Icheon, South Korea. From 2014 to 2018, he was a Circuit Design Engineer with Maxim Integrated Products Inc., Beaverton, OR. He is currently an Assistant Professor of electrical engineering with Daegu University, Gyeongbuk, South Korea. His research interests include low power ADC, CMOS RF modeling, and memory.

DAEWOONG KANG received the Ph.D. degree in electrical engineering from Seoul National University, Seoul, in 2009. From 2000 to 2015, he was with Samsung Electronics Company Ltd., Yongin, South Korea, where he was in charge of developing 2-D/3-D NAND flash as a PI Principal Engineer. From 2015 to 2019, he was a Senior Technologist (Principal) with Western Digital Corporation (WDC), San Jose, USA. From 2019 to 2022, he was a NAND Product Vice President (VP) with SK-Hynix Semiconductor, Icheon, South Korea, where he has developed the vertical NAND flash product with 128 layers for the first time in the world. His current research interests include the NAND process integration, cell characteristics, and reliability of 3-D flash memory.